.Physicochem. Probl. Miner. Process., 62(3), 2026, 224952

http://www.journalssystem.com/ppmp

Physicochemical Problems of Mineral Processing

ISSN 1643-1049

Experimental study on the separation performance of a self-adaptive hydrocyclone with overflow adjustment

Xinran Liu [1], Bo Chen [2], Can Li [2], Lanyue Jiang [2]

[1] School of Future Technology, South China University of Technology, Guangzhou 511442, China

[2] College of Mechanical and Electronic Engineering, Shandong University of Science and Technology, Qingdao 266590, China

Corresponding author: 13695422996@139.com (Xinran Liu)

Abstract: To address the issue of coarse particle mismatch in the overflow, this study proposes a self-adaptive hydrocyclone with overflow adjustment. By designing a conical vortex finder and a spring-loaded ball back pressure structure to achieve a size-adaptive adjustment of the vortex finder based on separation conditions. This study conducted a single-factor experiment to investigate the effects of feed pressure, feed concentration, and underflow port diameter on the separation performance of the hydrocyclone. The test results show: The centrifugal force within the hydrocyclone strengthened as the feed pressure increased, the solid yield of the underflow increased, and the separation efficiency curve shifted to the left. As the feed concentration rose, the content of coarse particles in the overflow increased, the cut size increased by 2.4 μm, and the separation performance decreased significantly. The hydrocyclone exhibits a high separation efficiency when the underflow port diameter is 12 mm.

Keywords: hydrocyclone, overflow adjustment, separation performance, back pressure, experimental study

1. Introduction

Hydrocyclones are widely used in many industries such as petrochemicals, coal, food processing, and water treatment due to their advantages, including simple structure, easy operation, high processing capacity, and low operating costs (César et al. 2024; Ji et al. 2023; Liu et al. 2023; Niazi et al. 2017). However, constrained by the structure and characteristics of hydrocyclones, coarse particle mismatch in the overflow is unavoidable in the separation process, particularly in grinding and classification operations. Consequently, it significantly increases the processing load of subsequent beneficiation operations and reduces the recovery efficiency of valuable minerals (Chu et al. 2022; da Silva et al. 2020). In addition, fluctuations in the concentration and particle size of in-feed materials are common in continuous production processes, which introduce further uncertainty into the particle separation of hydrocyclones and hinder their widespread implementation (Fang et al. 2023; Oats et al. 2010). Therefore, the design of an adaptive hydrocyclone to achieve automatic adjustment for fluctuations in feed materials is beneficial for stabilizing the production conditions and improving particle separation efficiency.

To address these issues, researchers have conducted extensive studies on various aspects of hydrocyclones, including structural, material, and operational parameters, to improve their separation efficiency (Çerik et al. 2022; Hembrom et al. 2018; Wang et al. 2022). Liu et al. (2024) designed a cyclone separation column with a flat-bottom structure to enhance the re-circulation effect at the bottom of the cyclone, which significantly reduced the mismatch of coarse particles in the overflow. Han et al. (2019) designed an internal cone & cylinder structure at the bottom of the hydrocyclone, and the experimental results showed that the design had no impact on the separation efficiency. But it notably reduced the separation pressure drop and stabilized the flow within the hydrocyclone. Jiang et al. (2019) reached a similar conclusion regarding their design of an adjustable underflow port structure. Cui et al. (2020) and Zhang et al. (2019) discovered that an appropriate increase in feed concentration could help to reduce the content of coarse particles in the overflow, while an appropriate increase in the underflow

DOI: 10.37190/ppmp/224952

port diameter could help to mitigate the negative impact of feed fluctuations on the particle separation process. Ghodrat et al. (2016) considered the interaction between particle size and density and used numerical simulation to investigate the classification and sorting process of particles within elongated and convex conical hydrocyclones, demonstrating that increasing the separation space within the conical section would improve separation efficiency, particularly by reducing the misplacement of light and coarse particles in the overflow. Tang et al. (2017) found that excessive feed pressure will increase turbulent disturbances in the overflow region, intensify the centrifugal force field, and affect the separation of coarse and fine particles, particularly those that are more likely to be entrained by the external swirl flow into the underflow.

The vortex finder functions as the direct outlet for fine-particle and low-density products; variations in its shape and parameters have a significant impact on the separation process (Su et al. 2022; Y. Wang et al. 2020; Yohana et al. 2022). Regarding the shape of the vortex finder, Li et al. (2025) designed a structure of a ring-shaped gap to divert the short-circuit flow into underflow, effectively reducing coarse-particle mismatch in the overflow. Jiang et al. (2018) reached similar conclusions by designing an arc-shaped vortex finder to achieve wall-guided flow of the short-circuit flow. Zhao et al. (2019) found through simulation that a design with vortex finders could reduce the separation pressure drop, minimize short-circuit flow and re-circulation flow, but would, to some extent, reduce the separation efficiency for particles of the median size. Chen et al. (2024) designed a three-product hydrocyclone with overflow re-separation, which utilizes the residual pressure from the overflow to perform a secondary separation, by removing mismatched particles that enter the overflow due to short-circuit flow and insufficient separation precision through a side overflow, a purer and finer central overflow is obtained. In addition, the relationship between the vortex finder diameter and insertion depth is a critical focus in studies on the separation efficiency of hydrocyclones. Zhang et al. (2023) found that static pressure, pressure drop, and the flow ratio exhibit a negative correlation with the vortex finder diameter, with reduced vortex finder diameter leading to a decrease in short-circuit flow, though separation energy consumption increases slightly. A simulation study by Tang et al. (2015) found that the factors affecting the separation efficiency of a cyclone, ranked by importance, are diameter, insertion depth, and wall thickness, respectively, and based on the computational results, a mathematical model was established to describe the influence of these parameters on separation efficiency.

Back pressure in a hydrocyclone refers to the opposing resistance pressure exerted on the outlets, which can be achieved by adjusting the discharge valve or designing functional structures. The presence of back pressure is beneficial for stabilizing the internal flow field, regulating the distribution of separated products, and reducing the mismatch of coarse particles in the overflow (Ni et al. 2016; Shang et al. 2024; Tian et al. 2019). Piller et al. (2016) observed that the presence of back pressure could enhance the re-circulation effect within the hydrocyclone, where a slight increase in local re-circulation contributes to improved separation efficiency, whereas excessive back pressure can substantially impact the outlet discharge. Tian et al. (2020) designed a back-pressure hydrocyclone for wastewater treatment applications, which enables intermittent discharge and re-circulation of the underflow by adjusting the back pressure and pressure-drop ratio, significantly enhancing the sludge concentration and separation efficiency. Sabbagh et al. (2017) installed an underflow pump, regulating the flow distribution of the outlet product via back pressure, which significantly improved the adaptability to feed fluctuations of the hydrocyclone. Liu et al. (2022) investigated the effect of overflow back pressure on the separation performance of a hydrocyclone, and the simulation results indicated that the total pressure drop increased with higher overflow back pressure, which resulted in greater separation energy consumption, an elevated solid-phase yield in the underflow, and significant particle mismatch in the underflow. Li et al. (2026) designed an adjustable hydraulic hydrocyclone by incorporating a flat plate into a conical vortex finder, which can effectively mitigate the stringy discharge and clogging of the underflow in high-concentration feed by adjusting the position and dimensions of the plate.

The aforementioned studies have provided methodological and directional guidance for the research presented in this paper. To address the issue of coarse particle mismatch in the overflow affecting the separation efficiency of hydrocyclones, this study proposes a self-adaptive hydrocyclone with overflow adjustment. By designing a conical vortex finder and a spring-loaded ball back pressure structure to achieve size-adaptive adjustment of the vortex finder based on operating conditions, which contributes

to enhancing particle separation efficiency and improving adaptability to fluctuations in feed conditions. This study conducted a single-factor experiment to investigate the effects of feed pressure, feed concentration, and underflow port diameter on the separation performance of an adaptive hydrocyclone. The findings would provide a theoretical basis for the industrial design and widespread application of hydrocyclones.

2. Research methodology

2.1. Design principle

In this study, based on ordinary hydrocyclone, the inner wall of the traditional cylindrical vortex finder is changed into a cone shape, and at the same time, a sphere and a spring are added, which adds an upward discharge resistance with overflow. When the feed properties change, it induces variations in the overflow back pressure, which in turn drives the ball to rise and fall within the vortex finder, altering the flow area of the overflow and adjusting the overflow flow rate. The elastic deformation of the spring is utilized to self-adapt to satisfy the change in pressure. The functions and structural diagrams of the adaptive cyclone are shown in Fig. 1 and Fig.2, with specific structural parameters listed in Table 1.

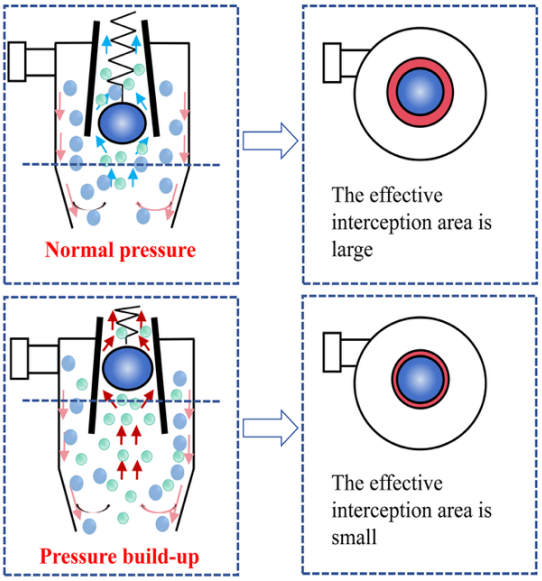

Fig. 1. Functional diagram of the self-adaptive hydrocyclone

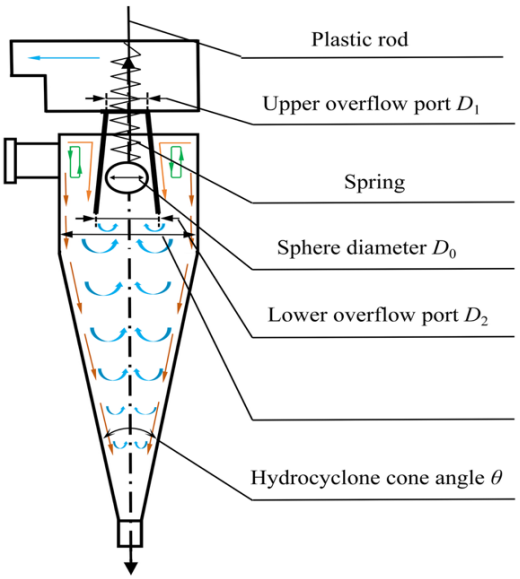

Fig. 2. Schematic diagram of a self-adaptive hydrocyclone

Table 1. The structure parameters of a self-adaptive hydrocyclone

Structure parameters	Size
Hydrocyclone diameter D /mm	75
Hydrocyclone cone angle θ /°	20
Upper overflow port D_1/mm	21
Lower overflow port D_2/mm	28
Sphere diameter D_0/mm	18
Spring wire diameter /mm	0.6
Spring Diameter /mm	12

2.2. Experimental design

This study conducted a single-factor experiment to investigate the effects of feed pressure, feed concentration, and underflow port diameter on the separation performance of the self-adaptive hydrocyclone. The experiments were conducted with hemispherical or printed spheres as test objects without considering their mass differences. A constant overflow circulation area was maintained by adjusting the position of the spheres, while the diameter of the upper end of the vortex finder was adjusted by changing the cone angle. Quartz sand and water were used as solid-liquid phases in the experiments, and three measurements of overflow and settled flow, mass, and volume were made to minimize errors and take average values. Conducting a full-scale experiment requires a large number of trials and a huge amount of work. A single-factor multistage test was conducted to determine the effect of a single factor on the separation performance, i.e., varying one factor while keeping other parameters constant. The table of factor levels used in the single-factor multilevel test is shown in Table 2. Meanwhile, the separation performance was analyzed in this paper using the concentration, solid yield & split ratio of underflow, particle size of separation products, and separation efficiency as evaluation indices.

Table 2. Experimental factors and parameters

Experimental factors	Parameters
Feed pressure（MPa）	0.06、0.08、0.10、0.12、0.14
Feed concentration（%）	7、10、13、16、19
Underflow port diameter（mm）	6、8、10、12、14

2.3. Experimental system

Employing closed-circuit operation to facilitate sampling and observation, the process began with preparing a solid-liquid mixture of specified concentration, which was homogenized in the mixing tank and fed into the hydrocyclone via the slurry pump; subsequently, both underflow and overflow products were recirculated to the mixing tank. The pump flow rate was adjusted using the variable-frequency control to achieve the designated feed pressure, and following parameter determination, the system maintained stable operation for a set duration, with multiple sampling rounds and comparative result analysis minimizing experimental error. Upon system stabilization, designated quantities of separated products were collected from the recirculation line, underflow outlet, and vortex finder. Fig 3 shows a physical diagram of the test system and the adaptive hydrocyclone. Mass concentrations of feed, overflow, and underflow products were determined through oven-drying and weighing, and performance metrics, including product size and separation efficiency, were quantitatively assessed.

2.4. Experimental material

In this experiment, a certain concentration of pulp was prepared by using water as the liquid phase (density of 998 kg/m^3) and quartz powder of 98% purity as the solid phase (mainly composed of S_iO_2,

density of 2650 kg/m^3). The composition and distribution of the feed particles were determined using a Malvern laser particle size analyzer, as shown in Fig. 4. Experiments employed batch-matched quartz sand and adopted a robust three-repetition particle size distribution (PSD) test to minimize the impact of particle shape on separation performance.

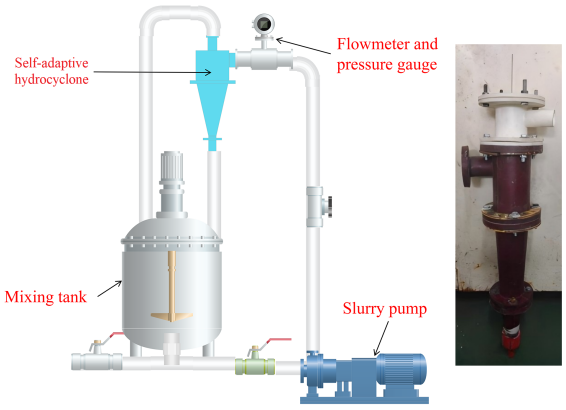

Fig. 3. Test system and self-adaptive hydrocyclone

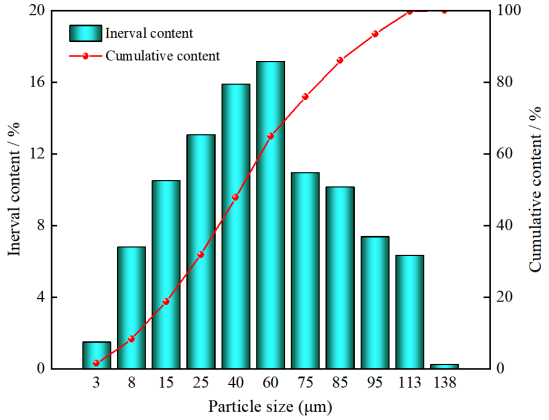

Fig. 4. Distribution of feed particles

3. Results and discussion

3.1. Effect of feed pressure on separation performance

To determine the feed concentration is 10%, the underflow port diameter is 10mm, and analyze the effect of feed pressure on the separation performance of the self-adaptive hydrocyclone when the feed pressure is 0.06MPa, 0.08MPa, 0.1MPa, 0.12MPa, and 0.14MPa, and the results are shown in Fig. 5-9.

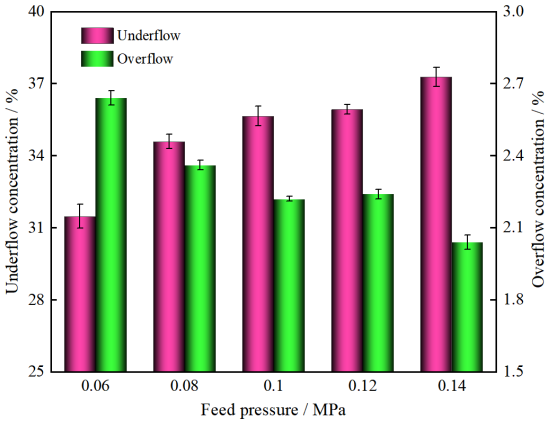

Fig. 5. Effect of pressure on product concentration

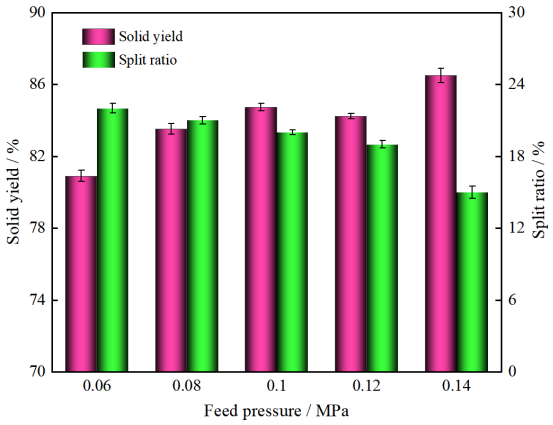

Fig. 6. Effect of pressure on solid yield and split ratio

Fig. 5 and Fig. 6 show the effect of feed pressure on product concentration, the underflow solid yield, and split ratio, respectively. As shown in Fig. 5, with the increase of feed pressure and centrifugal force, the overflow concentration decreases, and the underflow concentration rises from 31.28% to 37.48%. In the interval of feed pressure from 0.08 MPa to 0.12 MPa, the concentration did not change much, and the overflow concentration decreased from 2.64% to 2.04%. As shown in Fig. 6, as the feed pressure increased, the underflow solid yield increased from 80.91% to 86.49%, and at a pressure of 0.12 MPa, the underflow phase yield decreased, and the split ratio decreased from 22% to 17%. The aforementioned data indicate that when the pressure is low at 0.06 MPa, the centrifugal force is insufficient to drive normal particle classification, resulting in low underflow concentration and solid yield. Once the pressure reaches 0.12 MPa, further pressure increases will intensify the flow field within the hydrocyclone, affecting the residence time of particles during separation, resulting in an increase of particle content and a sharp decrease in the flow ratio. Furthermore, this leads to a hydraulic overload and impairs the functional realization of the adaptive structure.

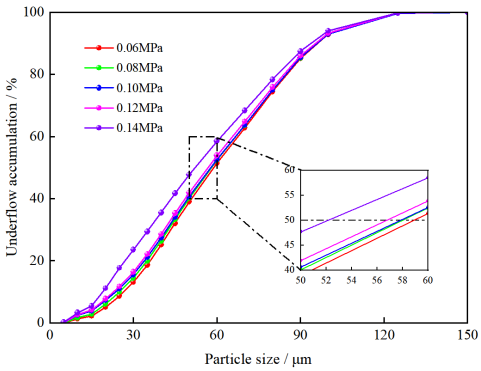

Fig. 7. Effect of pressure on underflow particle

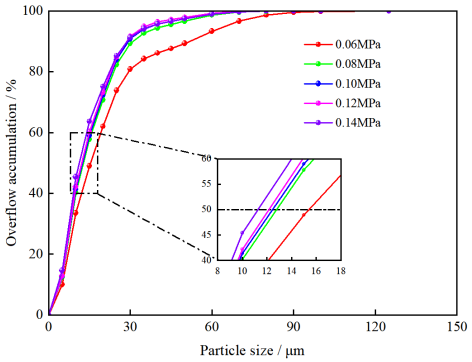

Fig. 8. Effect of pressure on overflow particle

Fig. 7 and Fig. 8 show the effect of feed pressure on the negative cumulative content of the product particle size of the self-adaptive hydrocyclone. With the increase of feed pressure from 0.06MPa to 0.14MPa, the negative cumulative content of particles in the underflow and overflow curves is shifted to the left. With the increase of feed pressure, the centrifugal force field within the hydrocyclone is strengthened, and some of the fine particles are migrated by centrifugal force to the outer cyclone to be discharged from the underflow port, the solid yield of the underflow rises, and the particle size of the underflow becomes finer. The content of coarse particles in the overflow decreases, and the overflow also becomes finer. It can also be observed that the underflow curve shifts significantly when the pressure increases from 0.12 MPa to 0.14 MPa, while the overflow curve shifts significantly when the pressure increases from 0.06 MPa to 0.08 MPa. This indicates that, under the designed parameters of the self-adaptive hydrocyclone, the separation performance remains relatively stable at pressures ranging from 0.08 to 0.12 MPa.

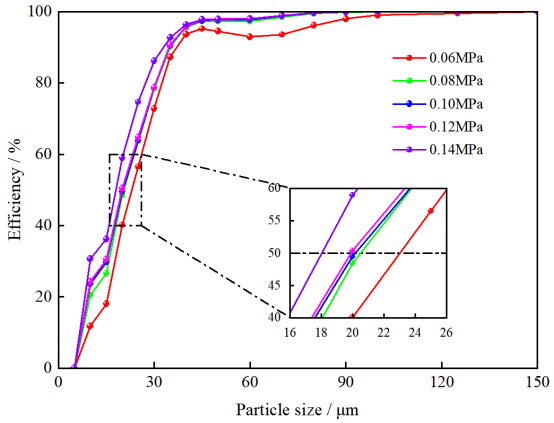

Fig. 9. Effect of pressure on classification efficiency

Fig. 9 shows the effect of feed pressure on the separation efficiency curve of the self-adaptive hydrocyclone. As the feed pressure increased from 0.06 MPa to 0.14 MPa, the separation efficiency curve shifted to the left, the cut size of the self-adaptive hydrocyclone decreased from 23 μm to 18 μm, and the recovery of each particle in the underflow increased.

3.2. Effect of feed concentration on separation performance

To determine the feed pressure of 0.1MPa, and the underflow port diameter is 10mm. Analyze the effect of feed concentration on the separation performance of the self-adaptive hydrocyclone when the feed concentration is at 7%, 10%, 13%, 16%, and 19%. The results are shown in Fig. 10-14.

As shown in Fig. 10, the product concentration has a direct relationship with the feed concentration. The feed concentration increases from 7% to 19%, the underflow concentration increases from 26.71%

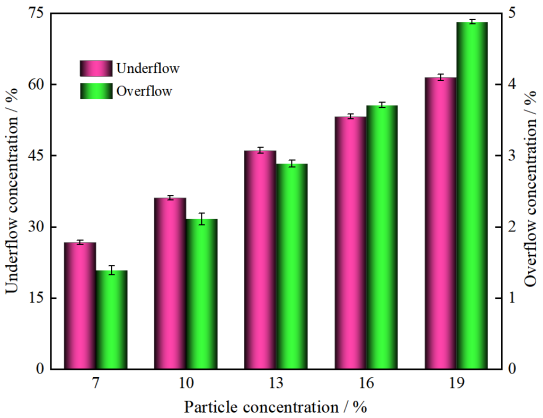

Fig. 10. Effect of feed concentration on product concentration

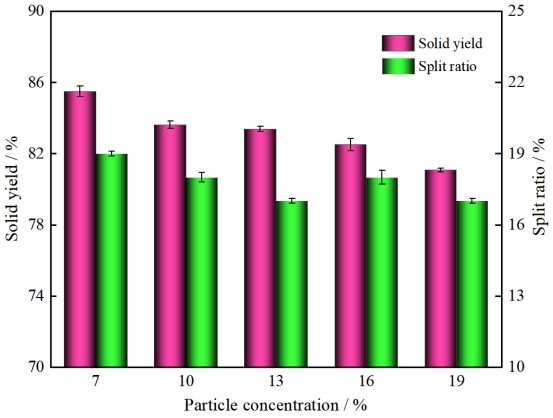

Fig. 11. Effect of feed concentration on solid yield and split ratio

to 61.46%, and the overflow concentration increases from 1.39% to 4.88%. Due to the spring and ball in the vortex finder to control the overflow's retention area, the resistance to overflow increases, which makes more flow to the underflow, so that the underflow concentration increases more obviously. Fig. 11 shows the effect of feed concentration on the underflow solid yield and split ratio. As the concentration increases from 7% to 19%, the underflow solid yield decreases from 85.5% to 81.08%, and the split ratio basically remains unchanged, keeping floating above and below 18%. With the increase of feed concentration, the underflow yield decreases in accordance with the law. As the feed concentration increases, the viscosity of the slurry increases, and the interactions between particles become bigger. The pressure of the internal flow field increases, pushing the ball upward, resulting in a reduction in the overflow circulation area, increasing overflow resistance, forcing the slurry to maintain a stable proportion of underflow discharge, so that the split ratio is basically unchanged.

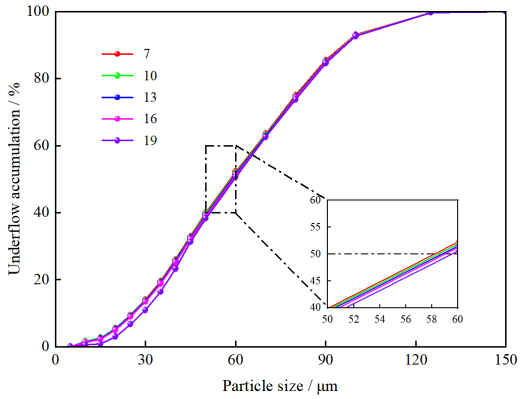

Fig. 12. Effect of feed concentration on underflow particle

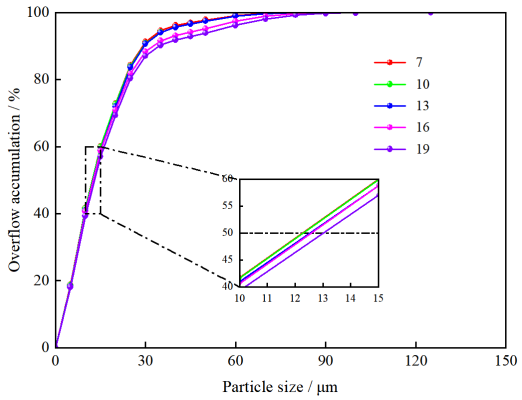

Fig. 13. Effect of feed concentration on overflow particle

Fig. 12 and Fig.13 show the effect of feed concentration on the negative cumulative content of product particle size. As the concentration increased from 7% to 19%, the negative cumulative curves of particle size in both underflow and overflow shifted to the right, and the content of -25 μm fine particles in the underflow decreased from 9.49% to 6.7%, and the content of +45 μm coarse particles increased from 66.99% to 68.8%. The content of -25μm fine particles in the overflow product decreased from 84.33% to 80.36%, and the content of +45μm coarse particles increased from 3% to 7.18%.

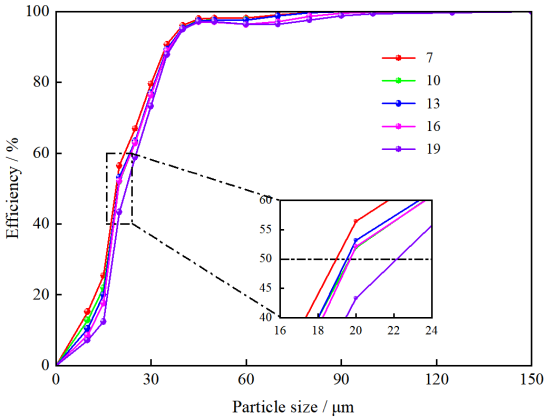

Fig. 14. Effect of feed concentration on classification efficiency

The effect of feed concentration on the classification efficiency curve is shown in Fig. 14. As the feed concentration increases, the interaction between the particles increases, and more fine particles enter the underflow. The classification efficiency curve shifts to the right, the recovery of +45 μm particles decreases with the increase of feed concentration, and the cut size increases from 19.7 μm to 22.1 μm.

3.3. Effect of underflow port diameter on separation performance

To determine the feed concentration of 11%, the feed pressure is 0.1 MPa. Analyze the effect of the size of the underflow opening diameter on the separation performance of the self-adaptive hydrocyclone when the underflow port diameter is 6mm, 8mm, 10mm, 12mm, and 14mm. The results are shown in Fig. 15-19.

Fig. 15 shows the effect of the underflow port diameter on the product concentration. As the underflow port diameter increases from 6 mm to 14 mm, the underflow concentration decreases from 48.06% to 23.47%, and the overflow concentration decreases from 2.41% to 2.2%. The increase in underflow port diameter certainly increases the particle and liquid in the underflow, and the concentration decreases because more particles flow out from the underflow, so the overflow concentration also decreases. Fig. 16 shows the effect of underflow port diameter on solid yield and split ratio. As the underflow opening increases from 6mm to 12mm, the underflow solid yield increases from 81.28% to 87.16%, and the split ratio increases from 11% to 31%. But when the diameter increases from 12mm to 14mm, the underflow phase yield and the split ratio decrease slightly.

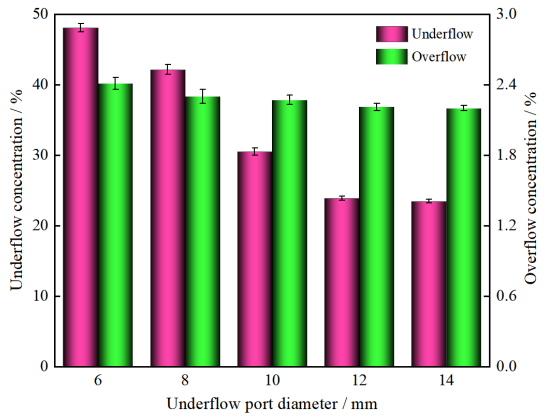

Fig. 15. Effect of underflow port diameter on product concentration

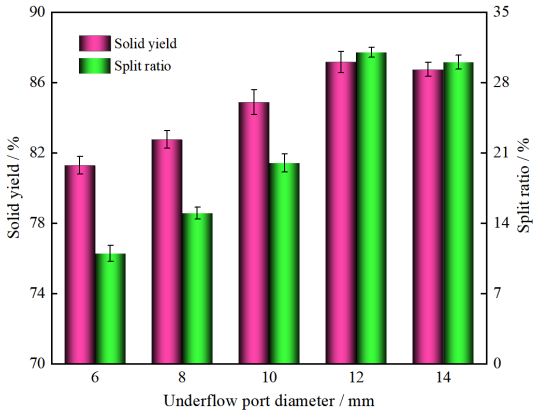

Fig. 16. Effect of underflow port diameter on solid yield and split ratio

Fig. 17and Fig. 18 show the effect of the underflow port diameter on the cumulative content of the product particles. As shown in Fig. 17, as the underflow port diameter increases, the underflow emission resistance decreases, more fine particles enter the underflow, and the effect is more pronounced as the particle size becomes finer. As shown in Fig. 18, with an increase of the underflow port diameter, the overflow curve shows minimal change. This is because the design structure can partially counteract the flow field disturbances caused by changes in the underflow port diameter, effectively reducing the mismatch of coarse particles in the overflow. The self-adapting hydrocyclone can achieve a fine-grained overflow product under various discharge ratios.

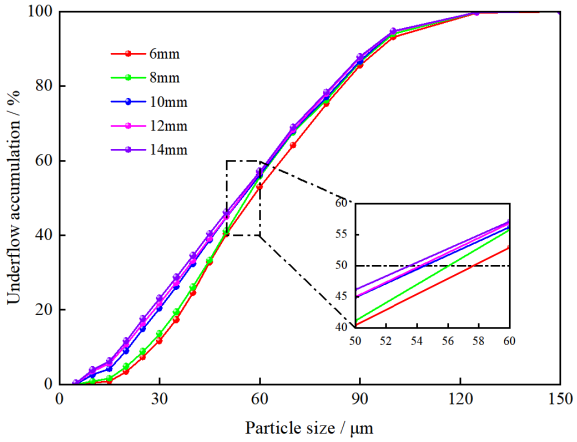

Fig. 17. Effect of underflow port diameter on underflow particle

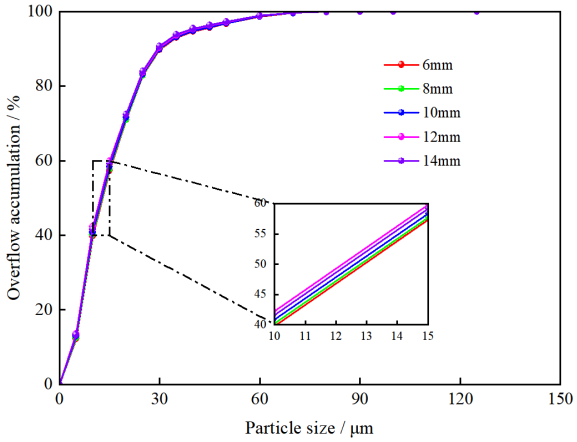

Fig. 18. Effect of underflow port diameter on overflow particle

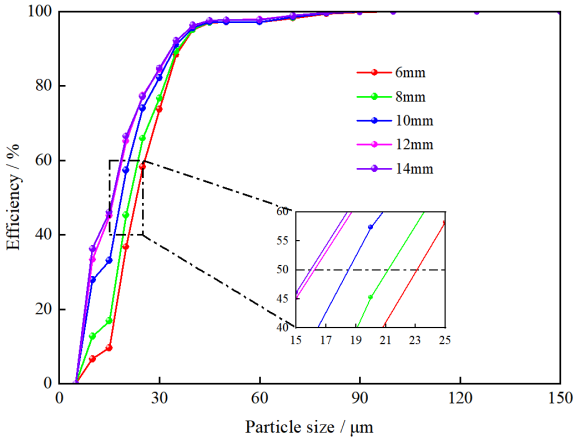

Fig. 19. Effect of underflow port diameter on classification efficiency

Fig. 19 shows the influence of the underflow port diameter on the separation efficiency curve. The curve shifts to the left when the underflow port diameter increases from 6mm to 14mm. With the increase in the underflow port diameter of the self-adaptive hydrocyclone, the underflow recovery of all particle sizes increases, and the cut size decreases from 22μm to 20.9 μm. Increasing the underflow port diameter appropriately can enhance the particle separation efficiency. However, when the diameter increases from 12 mm to 14 mm, finer particles begin to be mismatched in the underflow, which adversely affects the separation performance of the self-adaptive hydrocyclone.

4. Conclusions

To reduce the mismatch of coarse particles in the overflow, this paper proposes a self-adaptive hydrocyclone with overflow adjustment. A single-factor experiment was conducted to investigate the effects of feed pressure, feed concentration, and underflow port diameter on the separation performance of the hydrocyclone. The main conclusions are as follows：

(1) The centrifugal force within the self-adaptive hydrocyclone strengthened as the feed pressure increased. With the pressure raised from 0.06 MPa to 0.14 MPa, the solid yield of the underflow increased from 80.91% to 86.49%, the cut size decreased from 23 μm to 18 μm, the separation efficiency curve shifted to the left, and the separation efficiency for fine particles improved.

(2) The separation performance of the self-adaptive hydrocyclone decreases significantly as the feed concentration increases. With the feed concentration rising from 7% to 19%, both the concentration of underflow and overflow increased, and the underflow solid yield decreased from 85.5% to 81.08%. As the content of coarse particles in the overflow increased, the separation efficiency curve shifted to the right, and the cut size increased from 19.7 μm to 22.1 μm.

(3) The dimensional change of the underflow port diameter significantly affects the distribution of separation products. The dimension increased from 6mm to 12 mm, resulting in a rise in the split ratio of 20% and an increase in the underflow solid yield from 81.28% to 87.16%. The underflow particles gradually became finer, but further increasing them led to a decline in the separation performance of the self-adaptive hydrocyclone.

References

ÇERIK, Ç., ARSLAN, V., 2022. *The Modelling of Fine Coal Beneficiation with a Water-Only Cyclone*. Gospod. Surowcami Miner. / Miner. Resour. Manag. 38(3): 137–150.

CÉSAR, S.D., DEBBIE.D.J., NJOYA, M., 2024. *The Role of Hydrocyclone and Induced Gas Flotation Technologies in Offshore Produced Water Deoiling Advancements*. Pet. Res. 10(2): 342-351.

CHEN, B., LIU, P.K., GAO, Z.Z., JIANG, L.Y., HOU, D.X., WANG, F.Y., 2024. *Study on the Separation Performance of a Three-Product Hydrocyclone with Overflow Reseparation*. Powder. Technol. 448(579): 120303.

CHU, K.W., CHEN, Y.X., JI, L., ZHOU, Z.Q., YU, A.B., CHEN, J., 2022. *Coarse-Grained CFD-DEM Study of Gas-Solid Flow in Gas Cyclone*. Chem. Eng. Sci. 260: 117906.

CUI, B.Y., ZHANG, C.E., ZHAO, Q., HOU, D.X., WEI, D.Z., FENG, Y.Q., 2020. *Study on Interaction Effects between the Hydrocyclone Feed Flow Rate and the Feed Size Distribution*. Powder. Technol. 366: 617–628.

FANG, X., WANG, G.R., ZHONG, L., WANG, D.F., QIU, S.Z., Li, X.S., 2023. *Analysis of Weakly Cemented Gas Hydrate Bearing Sediments: Particle Movement and De-Cementation Behavior in Hydrocyclone Separator*. Powder. Technol. 424: 118174.

GHODRAT, M., Qi, Z., KUANG, S. B., Ji, L., Yu, A. B., 2016. *Computational Investigation of the Effect of Particle Density on the Multiphase Flows and Performance of Hydrocyclone*. Miner. Eng. 90: 55–69.

HAN, T.L., LIU, H.Y., XIAO, H., Chen, A.Q., HUANG, Q.S., 2019. *Experimental Study of the Effects of Apex Section Internals and Conical Section Length on the Performance of Solid–Liquid Hydrocyclone*. Chem. Eng. Res. Des. 145: 12–18.

HEMBROM, A.A., Suresh, N., 2018. *Evaluation of the Performance of a Water-Only Cyclone for Fine Coal Beneficiation Using an Optimization Process. Energy Sources, Part A: Recovery* Util. Environ. Eff. 40(23): 2842–2852.

JI, L., PAUL, P., SHANBHAG, B.K., DIXON, I., KUANG, S.B., HE, L.Z., 2023. *Emerging Application of Hydrocyclone in Biotechnology and Food Processing*. Sep. Purif. Technol. 309: 122992.

JIANG, L.Y., LIU, P.K., YANG, X.H., ZHANG, Y.K., 2018. *Short-Circuit Flow in Hydrocyclones with Arc-Shaped Vortex Finders*. Chem. Eng. Technol. 41(9): 1783–92.

JIANG, L.Y., LIU, P.K., YANG, X.H., ZHANG, Y.K., WANG, H., XU, C.C., 2019. *Numerical Analysis of Flow Field and Separation Characteristics in Hydrocyclones with Adjustable Apex*. Powder. Technol. 356: 941–956.

LI, L., DAI, L., ZENG, L., ZHOU, P.H., LI, J.P., WANG, H.L., 2025. *Structure Optimization of a Hydrocyclone for Separation of Recycled Rubber Particles with Low-Density Difference*. Process Saf. Environ. Prot. 195(12): 106724.

LI, X.Y., HAO, Y.K., LI, A.J., LIU, P.K., JIANG, L.Y., TIAN, S.B., 2026. *Experimental and Numerical Study on the Hydrodynamics and Classification Performance of Overflow Adjustable Hydrocyclones*. Powder. Technol. 468(8): 121654.

LIU, P.K., FU, W.X., JIANG, L.Y., ZHANG, Y.K., LI, X.Y., CHEN, B., 2022. *Effect of Back Pressure on the Separation Performance of a Hydrocyclone.Powder*. Technol. 409(6): 117823.

LIU, P.K., HOU, D.X., ZHAO, Q., JIANG, L.Y., CUI, B.Y., YIN, W.B., 2024. *Research on the Separation Chamber Diameter Ratio of the Multi-Stage Hydrocyclone to Inhibit Particle Misplacement*. Adv. Powder. Technol. 35(4): 104418.

LIU, P.K., WANG, H., JIANG, L.Y., ZHANG, Y.K., YANG, X.H., LI, F., 2023. *Study on the Cleanliness of Super Clean Coal Prepared by Water-Only Cyclone*. Physicochem. Probl. Miner. Process. 59(3): 168129.

NI, L., TIAN, J.Y., ZHAO, J.N., 2016. *Feasibility of a Novel De-Foulant Hydrocyclone with Reflux for Flushing Away Foulant Continuously*. Appl. Therm. Eng. 103: 695–704.

NIAZI, S., HABIBIAN, M., RAHIMI, M., 2017. *Performance Evaluation of a Uniflow Mini-Hydrocyclone for Removing Fine Heavy Metal Particles from Water*. Chem. Eng. Res. Des. 126: 89–96.

OATS, W.J., OZDEMIR, O., NGUYEN, A.V., 2010. *Effect of Mechanical and Chemical Clay Removals by Hydrocyclone and Dispersants on Coal Flotation*. Miner. Eng. 23(5): 413–419.

PILLER, M., SCHENA, G., BELARDI, G., 2016. *Sensitivity of Dyna Whirlpool Hydrocyclone Operation to Applied Back-Pressure*. Int. J. Miner. Process. 154: 81–93.

SABBAGH, R., LIPSETT, M., KOCH, C., NOBES, D., 2017. *An Experimental Investigation on Hydrocyclone Underflow Pumping*. *Powder*. Technol. 305: 99–108.

SHANG, M. YAO, Y., KE, X.W., HUANG, Z., ZHOU, T., LYU, J.F., 2024. *Effect of Back Pressure on Gas-Solid Distribution Characteristics of Cyclone Distributor Applied in Powdered Coal-Fired Circulating Fluidized Bed Combustion System. Powder*. Technol. 431: 119039.

DA SILVA, J.T.T.B., ISABELE C.R., GUSTAVO, P.A., CARLOS, H., 2020. *Hydrocyclone Applied in the Physical Processing of Phosphate Concentrate Containing Rare Earth Elements*. Miner. Eng. 155: 106402.

SU, T.L., ZHANG, Y.F., 2022. *Effect of the Vortex Finder and Feed Parameters on the Short-Circuit Flow and Separation Performance of a Hydrocyclone*. Processes 10(4): 771.

TANG, B., XU, Y.X., SONG, X.F., SUN, Z., YU, J.G., 2017. *Effect of Inlet Configuration on Hydrocyclone Performance. Trans. Nonferrous*. Met. Soc. 27: 1645–1655.

TANG, B., XU, Y.X., SONG, X.F., SUN, Z., YU, J.G., 2015. *Numerical Study on the Relationship between High Sharpness and Configurations of the Vortex Finder of a Hydrocyclone by Central Composite Design*. Chem. Eng. J. 278: 504–516.

TIAN, J.Y., NI, L., SONG, T., SHEN, C., YAO, Y., ZHAO, J.N., 2019. *Numerical Study of Foulant-Water Separation Using Hydrocyclones Enhanced by Reflux Device: Effect of Underflow Pipe Diameter*. Sep. Purif. Technol. 215: 10–24.

TIAN, J.Y., WANG, H.L., LV, W.J., HUANG, Y., FU, P.B., LIU, Y., 2020. *Enhancement of Pollutants Hydrocyclone Separation by Adjusting Back Pressure Ratio and Pressure Drop Ratio*. Sep. Purif. Technol. 240: 116604.

WANG, C., WEI, L. B., CUI, G. W., 2022. *Effects of the Operating Parameters on the Separation Results of a Three-Stage Cone Water-Only Cyclone*. Int. J. Coal Prep. Util. 42(8): 2314–2331.

WANG, Y., CHANG, Y.Y., LI, J.P., WANG, H.L., LI, L.Q., YUAN, Y.P., 2020. *Analysis of Performance of Novel Hydrocyclones in Ebullated Bed Reactor with Different Vortex Finder Structures*. Chem. Eng. Res. Des. 158: 89–101.

YOHANA, E., TAUVIQIRRAHMAN, M., LAKSONO, D., CHARLES, H., CHOI, K., YULIANTO, M., 2022. *Innovation of Vortex Finder Geometry (Tapered in-Cylinder out) and Additional Cooling of Body Cyclone on Velocity Flow Field, Performance, and Heat Transfer of Cyclone Separator*. Powder. Technol. 399: 117235.

ZHANG, C.E., CUI, B.Y., WEI, D.Z., LU, S.S., 2019. *Effects of Underflow Orifice Diameter on the Hydrocyclone Separation Performance with Different Feed Size Distributions*. Powder. Technol. 355: 481–494.

ZHANG, Y.K., XU, M.Y., HU, W., XU, X.X., ZHANG, Q.Y., 2023. *Vortex Finder Diameter and Depth Effects on the Separation Performance of Hydrocyclone.* Chem. Eng. Res. Des. 195: 181–191.

ZHAO, Q., CUI, B.Y., WEI, D.Z., SONG, T., FENG, Y.Q., 2019. *Numerical Analysis of the Flow Field and Separation Performance in Hydrocyclones with Different Vortex Finder Wall Thickness*. Powder. Technol. 345: 478–491.